

MOL #37150

Inhibition of TRPP3 channel by amiloride and analogs

Xiao-Qing Dai, Alkarim Ramji, Yan Liu, Qiang Li, Edward Karpinski, and Xing-Zhen Chen*

Membrane Protein Research Group, Department of Physiology, University of Alberta, Edmonton,
Alberta, T6G 2H7, Canada

Running title: Inhibition of TRPP3 by amiloride analogs

***Corresponding author:**

Dr. Xing-Zhen Chen

729 Medical Science Building

Department of Physiology

University of Alberta

Edmonton, Alberta, T6G 2H7, Canada

Tel: 1-780-492-2294

Fax: 1-780-492-8915

Email: xzchen@ualberta.ca

Number of Text Pages:	24
Number of Figures:	8
Number of References:	35
Number of words in Abstract:	248
Number of words in Introduction:	642
Number of word in Discussion:	1280

List of Abbreviations

ADPKD: autosomal dominant polycystic kidney disease; ARPKD, autosomal recessive polycystic kidney disease; TRPP2: transient receptor potential polycystin-2; TRPP3: transient receptor potential polycystin-L; TRPP5: transient receptor potential polycystin-2L2; EIPA: 5-(*N*-ethyl-*N*-isopropyl) amiloride; TPeA: tetra-pentylammonium

Abstract

TRPP3, a member of the transient receptor potential (TRP) superfamily of cation channels, is a Ca-activated channel permeable to Ca, Na and K. TRPP3 has been implicated in sour tasting in bipolar cells of tongue and in regulation of pH-sensitive action potential in spinal cord neurons. TRPP3 is also present in excitable and non-excitable cells of other tissues, including retina, brain, heart, testis and kidney, with unknown functions. Here we examined the functional modulation of TRPP3 channel by amiloride and its analogs, known to inhibit several ion channels and transporters and respond to all taste stimuli, using *Xenopus* oocytes expression, electrophysiology and radiotracer measurements. We found that amiloride and its analogs inhibit TRPP3 channel activities with different affinities. Radiolabelled ^{45}Ca uptake showed that TRPP3-mediated Ca transport is inhibited by amiloride, phenamil, benzamil and EIPA. Two-microelectrode voltage clamp experiments revealed that TRPP3-mediated Ca-activated currents are substantially inhibited by amiloride analogs, in an order of potency of phenamil > benzamil > EIPA > amiloride, with the IC_{50} values of 0.14, 1.1, 10.5 and 143 μM , respectively. The inhibition potency positively correlated with the size of inhibitors. Using cell-attached patch clamping, we showed that the amiloride analogs decrease the open probability and mean open time, but have no effect on single-channel conductance. Study of inhibition by phenamil in the presence of previously reported inhibitor tetrapentylammonium indicates that amiloride and organic cation inhibitors compete for binding the same site on TRPP3. TRPP3 may contribute to previously reported *in vivo* amiloride-sensitive cation transport.

Introduction

TRPP3 (also called polycystin-L), initially cloned from human retina EST (Nomura *et al.*, 1998; Wu *et al.*, 1998), is a novel member of the transient receptor potential (TRP) superfamily of cation channels. TRPP3 has two homologs, TRPP2 (or polycystin-2) and TRPP5 (or polycystin-2L2), which share amino acid sequence similarity of ~70%. TRPP2 is part of a flow sensor and its mutations account for ~10% of autosomal dominant polycystic kidney disease (ADPKD), while the function and physiological roles of TRPP5 remain unknown. TRPP3 is localized to a subset of taste receptor cells in the tongue where it may play a crucial role in sour tasting (Huang *et al.*, 2006; Ishimaru *et al.*, 2006; LopezJimenez *et al.*, 2006), and to neurons surrounding the central canal of the spinal cord where it may account for the long-sought proton-dependent regulation of the frequency of action potential (Huang *et al.*, 2006). TRPP3 is present in neuronal or non-neuronal (eg epithelial) cells of other tissues, such as kidney, heart, retina, testis, liver, pancreas, and spleen (Basora *et al.*, 2002). In fact, TRPP3 is found in the ganglion cells of retina and collecting duct epithelial cells of kidney. We recently also revealed that TRPP3 is present in photoreceptor cells of mouse retina (unpublished data). However, the function of TRPP3 in retina has not been reported. It is thus interesting to determine whether there exists a common mechanism underlying its physiological roles in various tissues.

TRPP3 is a Ca-activated non-selective cation channel permeable to Ca, K, Na, Rb, NH₄, and Ba, inhibited by Mg, H, La and Gd (Chen *et al.*, 1999; Liu *et al.*, 2002). Based on its permeability to monovalent organic cations (methlyamine, dimethylamine and triethylamine and tetramethylammonium) and inhibition by larger compounds tetra-ethylammonium, tetrapropylammonium, tetra-butylammonium and tetra-pentylammonium, a pore size of ~7 Å was estimated (Dai *et al.*, 2006). TRPP3 is not a voltage-gated channel but its channel properties show significant voltage-dependence (Chen *et al.*, 1999; Liu *et al.*, 2002). Interestingly, co-expression of

TRPP3 with polycystin-1, a large receptor-like membrane protein mutated in 80-85% of ADPKD, in human embryonic kidney (HEK) 293 cells resulted in TRPP3 trafficking to the plasma membrane, where TRPP3 seemed to mediate Ca entry in the presence of a hypo-osmotic extracellular solution (Murakami *et al.*, 2005). Co-expression of mouse TRPP3 and polycystin-1L3, an isoform of polycystin-1 with unknown function, but not the expression of TRPP3 or polycystin-1L3 alone, also target to the plasma membrane of HEK 293 cells and mediate pH-activated cation conductance (Ishimaru *et al.*, 2006). Whether the presence of polycystin-1L3, cell type and/or species difference account for the observed opposite pH dependence of TRPP3 function remain to be elucidated (Chen *et al.*, 1999; Ishimaru *et al.*, 2006). On the other hand, TRPP2 is a Ca-permeable non-selective cation channel involved in ER Ca homeostasis (Gonzalez-Perret *et al.*, 2001; Koulen *et al.*, 2002), and together with polycystin-1, forms a channel complex which acts as part of flow sensor in renal epithelial primary cilia (Nauli *et al.*, 2003). Thus, like other TRP members, TRPP2 and TRPP3 are likely to be part of cellular sensors (Clapham, 2003).

Amiloride (or *N*-amidino-3,5-diamino-6-chloropyrazinecarboxamide) and its analogs, such as 5-(*N*-ethyl-*N*-isopropyl) amiloride (EIPA), benzamil and phenamil (Fig. 1A), have been extensively used as probes for a wide variety of transport systems (Kleyman & Cragoe, Jr., 1988). Amiloride is a well known antagonist of ENaC, Na/Ca and Na/H exchangers, non-selective cation channels, and voltage-gated K and Ca channels (Doi & Marunaka, 1995; Hirsh, 2002; Kleyman & Cragoe, Jr., 1988; Kleyman & Cragoe, Jr., 1990; Murata *et al.*, 1995; Sariban-Sohraby & Benos, 1986; Stoner & Viggiano, 2000; Tytgat *et al.*, 1990). Interestingly, amiloride has been reported to inhibit all types of taste responses (sweet, bitter, umami, salty and sour) (Gilbertson *et al.*, 1993; Lilley *et al.*, 2004). In this study we examined the inhibitory effects of amiloride analogs on TRPP3, using *Xenopus* oocyte expression in combination with whole-cell and single-channel electrophysiology, as well as radiotracer uptake measurements.

Materials and Methods

Oocyte preparation

Capped synthetic human TRPP3 mRNA was synthesized by *in vitro* transcription from a linearized template, using the mMESSAGE mMACHINE1 Kit (Ambion, Austin, TX, USA). Stage V-VI oocytes were extracted from *Xenopus laevis* and defolliculated by collagenase type I (2.5 mg/ml) (Sigma-Aldrich Canada, Oakville, ON, Canada) in the Barth's solution (in mM, 88 NaCl, 1 KCl, 0.33 Ca(NO₃)₂, 0.41 CaCl₂, 0.82 MgSO₄, 2.4 NaHCO₃, 10 HEPES, and pH 7.5) at room temperature for about 2 hr. Each oocyte was injected with 50 nl of RNase-free water containing 25 ng of TRPP3 mRNA 5-20 hr following defolliculation. An equal volume of RNase-free water was injected into each control oocyte. Injected oocytes were incubated at 18°C in the Barth's solution supplemented with antibiotics, penicillin-streptomycin (Gibco, Invitrogen Corporation, Grans Island, NY, USA) for 2-4 days prior to experiments. The animal experimentation was performed in accordance with the University of Alberta regulation concerning animal welfare.

⁴⁵Ca uptake measurement

Radiotracer uptake experiments were performed as previously described (Chen *et al.*, 1999). Briefly, the uptake solution was composed of the NaCl-containing solution (in mM: 100 NaCl, 2 KCl, 1 MgCl₂, 10 HEPES, pH 7.5) plus 1 mM non-radiolabelled CaCl₂ and 1:1000 radiolabelled ⁴⁵Ca with specific activity of 2 μCi/μl (Amersham Pharmacia Biotech, Montreal, QC, Canada). 10 oocytes were incubated in 0.5 ml of the uptake solution, for 30 min with gentle shaking from time to time. Uptake was terminated by washing oocytes in the ice-cold NaCl-containing solution. Amiloride, EIPA, benzamil and phenamil were purchased from Sigma-Aldrich Canada.

Two-microelectrode voltage clamp

Two-microelectrode voltage clamp was performed as described previously (Liu *et al.*, 2002; Li *et al.*, 2003). Briefly, the two electrodes (Capillary pipettes, Warner Instruments, Hamden, CT, USA) impaling *Xenopus* oocytes were filled with 3 M KCl to form a tip resistance of 0.3 ~ 3 M Ω . Oocyte voltages and whole-cell currents were recorded using an amplifier (Geneclamp 500B, Axon Instruments, Union City, CA, USA) and pClamp 9 software (Axon Instruments), and stored in a PC computer after AD/DA conversion (Digidata1320A, Axon Instruments). Currents and voltages were sampled at intervals of 200 μ s and filtered at 2 kHz using an 8 pole Bessel filter. In experiments using a ‘gap-free’ (continuous acquisition at a holding voltage) or ramp protocol (Fig. 2B, top), current/voltage signals were sampled at intervals of 0.2 or 200 ms, respectively. Standard NaCl-containing solution contained (in mM): 100 NaCl, 2 KCl, 0.2 MgCl₂, 10 HEPES, pH 7.5.

Patch clamp

The vitelline layer of oocytes was manually removed following incubation at room temperature in a hypertonic solution (Barth’s solution plus 200 mM sucrose). Oocytes were then transferred to a recording chamber with Barth’s solution and allowed to recover for 10 ~ 20 min before clamping. Electrodes were filled with a pipette solution containing 123 mM K (in mM: 110 KCl, 13 KOH, 10 HEPES, and pH 7.4) to form tip resistance of 3 - 8 M Ω . Single-channel currents were recorded in cell-attached configuration using PC-ONE Patch Clamp amplifier (Dagan Corp., Minneapolis, MN, USA), DigiData 1322A interface, and pClamp 9 software. Recording started after seal resistance reached at least 3 G Ω . Current and voltage signals were sampled every 200 μ s and filtered at 2 kHz.

Statistics and data analysis

Data obtained from the two-microelectrode voltage clamp and patch clamp experiments were analyzed using Clampfit 9. For single-channel event detection, automatic level update was used (with 10% contribution) and the threshold value was equal to 50% of the current amplitude. Single-channel conductance values were obtained from Gaussian fits to density plots (all-point histograms). The open probability times the number of channels in the patch (NP_o , designated 'open probability' hereafter) and channel mean open time (MOT) values were obtained from currents generated either by voltage pulses of 10 s per pulse or by gap-free recordings of 10 s long. For the MOT analysis, recordings with single openings were used without filtering. Analyzed data were plotted using Sigmaplot 9 (Jandel Scientific Software, San Rafael, CA, USA) and expressed in the form of mean \pm SE (N), where SE represents the standard error of the mean and N indicates the number of oocytes (or oocyte patches) tested. Data filtering and curve fitting were performed using Clampfit 9 and Sigmaplot 9, respectively. The diameters of amiloride and its analogs were measured with *Spartan* 4 (Wavefunction Inc, Irvine, CA, USA). Concentration-dependent curves were fitted with the 3-parameter Logistic equation: $I/I_{\max} = 1/[1 + ([B]/IC_{50})^{n_H}]$, where [B] represents the concentration of amiloride or its analog and n_H represents the Hill coefficient. Comparison between two sets of data was analyzed by *t*-test or two-way ANOVA, and a probability value (P) of less than 0.05 and 0.01 was considered significant and very significant, respectively.

Results

Inhibition of TRPP3-mediated ^{45}Ca uptake by amiloride and its analogs

We first utilized radiotracer uptake assays to assess the whole-cell Ca transport activities in *Xenopus* oocytes. Oocytes injected with TRPP3 mRNA exhibited increased Ca entry, compared to the control (H_2O -injected) oocytes. In the presence of 500 μM amiloride, 100 μM EIPA, 10 μM benzamil and 10 μM phenamil, ^{45}Ca uptake decreased from 79 ± 9 to 46 ± 4 (58% remaining), 27 ± 4 (34%), 29 ± 5 (37%), and 38 ± 4 (48%) pmol/oocyte/30 min ($N = 6$, $P = 0.008$), respectively (Fig. 1B). These compounds displayed little effects on the Ca transport of control oocytes, indicating that TRPP3-mediated Ca transport is significantly inhibited by amiloride and its analogs.

Inhibition of TRPP3-mediated whole-cell currents by amiloride analogs

We next employed the two-microelectrode voltage clamp technique to examine the inhibitory effects of amiloride and its analogs. In TRPP3-expressing oocytes, large inward currents were evoked by adding 5 mM Ca to the NaCl-containing solution at the holding potential of -50 mV. Currents were activated and reached a peak in 10 ~ 20 s after Ca was added and then inactivated. The Ca-activated TRPP3 inward current was reduced in the presence of extracellular amiloride at 100 μM ($40.3 \pm 8.6\%$ inhibition, $P = 0.0001$, $N = 18$) or 500 μM ($85.9 \pm 11.3\%$ inhibition, $P = 0.0005$, $N = 20$) (see eg Fig. 2A), but not at 10 μM ($P = 0.2$, $N = 13$), indicating a rather low-affinity inhibition. This inhibition by amiloride was reversible as the inward current recovered 8 ~ 10 min after washout (see representative tracing in Fig. 2A), which is also approximately the time required for evoking a second activation of the channel following the first activation (in the absence of amiloride) (Chen *et al.*, 1999). Using a ramp voltage protocol, we showed that amiloride also exhibits its inhibitory effect at other membrane potentials, as shown by averaged current-voltage curves obtained in the presence and absence of amiloride (Fig. 2B).

Because amiloride is a low-affinity inhibitor of the TRPP3 channel, we wondered whether its analogs have similar effects on TRPP3. We tested the effects of EIPA, benzamil and phenamil, which are formed by replacing one of the two amino groups in amiloride with more hydrophobic side chains (Fig. 1A). We found that EIPA, benzamil and phenamil rapidly and reversibly block Ca-activated TRPP3 channel activation at -50 mV as well as at other membrane potentials (Fig. 2C-F). When currents obtained at -50 mV in the presence of various concentrations of amiloride and its analogs were averaged and fitted with the Logistic equation (see Methods), we obtained the IC₅₀ values of 143 ± 8 (N = 36), 10.5 ± 2.2 (N = 28), 1.1 ± 0.3 (N = 30) and 0.14 ± 0.04 μM (N = 25) for amiloride, EIPA, benzamil and phenamil, respectively (Fig. 2G). Thus, the inhibition potency order is phenamil > benzamil > EIPA > amiloride, with the difference in affinity of roughly 10-fold between two consecutive inhibitors.

Our previous data showed that large TAA compounds, known as inhibitors of non-selective cation channels, inhibit TRPP3 (Dai *et al.*, 2006). To gain insight into whether these inhibitors bind to the same site as amiloride analogs we examined inhibition of phenamil in the presence of tetrapentylammonium (TPeA). We found that the IC₅₀ value for phenamil is 4.30 ± 0.02 μM in the presence of 0.5 μM TPeA (the IC₅₀ value for TPeA was 1.3 μM), which is 30-fold higher than the value in the absence of TPeA (Fig. 2H). These data suggest that the two classes of inhibitor compete for the same binding site in TRPP3.

In the absence of Ca, the basal Na current was also reversibly inhibited by 100 - 500 μM amiloride, 10 - 100 μM EIPA, 1 - 10 μM benzamil and 0.03 - 1 μM phenamil, with similar affinity constants (Fig. 3) compared to the inhibition of Ca-activated currents (Fig. 2G). With 500 μM amiloride, 100 μM EIPA, 10 μM benzamil or 1 μM phenamil, the basal Na currents of the TRPP3 channel were significantly and reversibly inhibited (Fig. 3A-C). The basal Na currents in H₂O-injected oocytes were not significantly inhibited by 500 μM amiloride or 1 μM phenamil (data not

shown). The IC_{50} values were 209, 19.5, 2.4 and 0.28 μM for amiloride, EIPA, benzamil and phenamil, respectively (Fig. 3D).

Inhibition of single-channel activities of TRPP3 by amiloride analogs

To examine inhibitory effects of amiloride analogs on TRPP3 single-channel activities we used the cell-attached mode of patch clamp. In the presence of 123 mM K in the pipette, TRPP3 channel openings were observed in 245 out of 296 patches in oocytes over-expressing TRPP3. With linear regression in negative ($-V_m$: -20 ~ -120 mV) and positive membrane potentials ($+V_m$: +20 ~ +120 mV), we calculated that TRPP3 has a larger inward single-channel conductance (399 ± 12 pS at $-V_m$, $N = 30$) than outward conductance (137 ± 10 pS at $+V_m$, $N = 26$), presumably due to inward rectification and the presence of asymmetrical concentrations of permeant ions on the two sides of the membrane (Liu *et al.*, 2002). No channel openings of similar main conductance were observed in H_2O -injected control oocytes ($N = 20$).

We performed cell-attached recordings in the presence or absence of pipette amiloride from patches of the same oocyte to minimize variations due to changes in the surface expression of different oocytes. At both positive and negative voltages, amiloride (500 μM) significantly decreased TRPP3 single-channel NP_o but not the amplitude (Fig. 4). A two-way ANOVA analysis revealed that 500 μM amiloride significantly inhibits NP_o ($P < 0.0001$) and that NP_o value is voltage-dependent ($P < 0.0001$), with higher NP_o values at $-V_m$ (Fig. 4B). The MOT values were also altered by extracellular amiloride ($P = 0.002$) and were voltage-dependent ($P < 0.0001$), with higher MOT values at $-V_m$ (Fig. 4C). Of note, no effect on NP_o and MOT was observed when 10 μM amiloride was added to the pipette solution, indicative of low-affinity inhibition by amiloride. Similarly, we found that EIPA, benzamil and phenamil, exhibit inhibitory effects on NP_o and MOT, but not on the single-channel amplitude (Fig. 5-7). The inhibition by EIPA was concentration-

MOL #37150

dependent and the IC_{50} values for EIPA inhibition on NP_o were 13.7 ± 1.5 and 18.1 ± 0.8 μM at -120 and +120 mV, respectively ($P < 0.01$, $N = 20$) (Fig. 5B). The IC_{50} values on MOT were 25 ± 4 and 28 ± 5 μM , respectively ($P < 0.01$, $N = 20$) (Fig. 5C). Those for benzamil on NP_o were 0.5 ± 0.01 and 1.4 ± 0.3 μM at -120 and +120 mV ($P < 0.01$, $N = 11$), respectively, while those on MOT were 0.8 ± 0.03 and 1.7 ± 0.3 μM , respectively ($P < 0.01$, $N = 13$) (Fig. 6B and C). Phenamil exhibited similar inhibition characteristics than its analogs but with higher potency. The IC_{50} values for phenamil on NP_o were 0.24 ± 0.04 and 0.39 ± 0.07 μM at -120 and +120 mV ($P < 0.05$, $N = 26$), respectively, while those on MOT were 0.45 ± 0.01 and 0.52 ± 0.08 μM , respectively ($P < 0.01$, $N = 19$) (Fig. 7B and C). The inhibition effects on NP_o , MOT and mean current by 500 μM amiloride, 100 μM EIPA, 1 μM benzamil and 1 μM phenamil at $-V_m$ and $+V_m$ were compared (Fig. 8A-C). Of note, we also examined the effects of intracellular amiloride analogs pre-injected 3 hr prior to experiments. No significant effect was observed (data not shown), suggesting that they do not exhibit similar inhibition from the intracellular side of the membrane.

Discussion

As a well-known blocker of ENaC, Na/Ca and Na/H exchangers, non-selective cation channels and voltage-gated K and Ca channels, amiloride also inhibits the responses to all taste stimuli (Gilbertson et al., 1993; Lilley et al., 2004), currents induced by the expression of polycystin-1 C-terminal fragments in *Xenopus* oocytes (Vandorpe et al., 2001), and those mediated by TRPP2 channels reconstituted in lipid bilayer or over-expressed in sympathetic neurons (Gonzalez-Perret et al., 2001; Delmas et al., 2004). Interestingly, recent reports showed that TRPP3 plays an important role in sour tasting and acid sensing (Huang et al., 2006; Ishimaru et al., 2006). TRPP3 is concentrated in the apical membrane (facing taste pores) of bipolar cells in taste buds, suggesting that it allows an initial cation influx triggered by low pH at the taste pore, which activates surrounding voltage-gated cation channels via local membrane depolarization and then leads to the firing of an action potential. In the whole length of the spinal cord, TRPP3 is present in neurons that project into the central canal, suggesting that it may also trigger an initial cation entry following a decrease in the canal pH (Huang et al., 2006). However, it remains unclear as to why TRPP3 responds to two very different pH ranges in the tongue and spinal cord. It is possible that polycystin-1L3 plays a role in acid sensing.

In the present study we investigated the modulation of the TRPP3 channel function by amiloride and its analogs (phenamil, benzamil and EIPA), using whole-cell and single-channel electrophysiology and radiotracer uptake measurements. These compounds inhibited both the Ca-activated and basal, TRPP3-mediated cation transports in *Xenopus* oocytes. In radiotracer uptake experiments, oocytes are not voltage clamped (to negative membrane potentials, eg -50 mV), any significant Ca entry will immediately lead to membrane depolarization, which slows down further Ca entry. Thus, Ca entry should not be sufficient in these experiments to induce TRPP3 channel activation and should reflect the basal TRPP3 channel activity. In cell-attached experiments,

because Ca was absent in the pipette solution, single-channel activities correspond also to the basal TRPP3 function. In fact, so far we have not been able to conclude as to whether Ca (5 mM) in the cell-attached pipette can induce activation of TRPP3 channels present in the patch. An important difference to the whole-cell voltage clamp may be that the Ca entry through the tiny membrane patch under the pipette does not cause sufficient increase in the local intracellular Ca concentration in the proximity of the patch to activate these few TRPP3 channels, due to fast diffusion of Ca ions.

Amiloride analogs are 2-3 fold more effective, as judged by IC_{50} values, in blocking the Ca-activated current than the basal current. This might be due to the possibility that amiloride analogs are more potent inhibitors for the current carried by Ca ions which are about 5 times more permeant to TRPP3 than Na (Chen *et al.*, 1999). Another possibility is that the proportion of current already inhibited by 1 mM Mg in the solution differs between the basal and activation conditions. These inhibitors reduce the NP_o and MOT, but not the single-channel conductance. Because no rapid ‘flickery’ block was observed, our data suggest that these inhibitors alter channel gating by binding to a site(s) on the channel protein outside the pore pathway, instead of competing with permeant ions such as Ca and Na.

Interestingly, the hydrophobicity of the side chain, the molecular diameter, and the inhibition potency of these analogs follow the same order, phenamil > benzamil > EIPA > amiloride (Fig. 8D), which is different from one for ENaC (phenamil > benzamil > amiloride > EIPA) and Na/H exchanger (phenamil > EIPA > amilorde, benzamil) (Kleyman & Cragoe, Jr., 1988), suggesting that these membrane proteins have different binding kinetics or structures for the inhibitors. It is possible that the binding cassette in TRPP3 has a hydrophobic environment that promotes binding of ligands of higher hydrophobicity or that the size of the binding cassette is closer to that of phenamil than the other inhibitors. We previously estimated that TRPP3 channel possesses a pore diameter of ~ 7 Å and a binding cassette of at least 13 Å for organic cation

inhibitors (Dai *et al.*, 2006). In that study we revealed that the largest inhibitor TPeA, with a size of ~13 Å, is most potent among the other organic cation inhibitors tested. We also found that these inhibitors, except tetra-butylammonium, reduce NP_o and MOT, but not the single-channel conductance. This raises the possibility that amiloride analogs and organic cation inhibitors share the same binding site. This is supported by our finding that the IC₅₀ value for phenamil augments by 30-fold in the presence of 0.5 μM TPeA.

Renal Na reabsorption is crucial for Na and body fluid homeostasis. Amiloride-sensitive Na reabsorption constitutes a major ion transport pathway in the principal cells of cystic and non-cystic collecting tubules (Hirsh, 2002). It was reported that amiloride-sensitive non-selective channels with unclear molecular identities may contribute to Na reabsorption in distal tubules, collecting ducts, cultured A6 kidney cells, hippocampus and Ehrlich-Lette-ascites tumour cells (Chu *et al.*, 2003;Lawonn *et al.*, 2003). Interestingly, TRPP3 is present in the apical region of renal principal cells (Basora *et al.*, 2002) and part of Na reabsorption in collecting ducts was reported to be mediated by amiloride-sensitive non-selective cation channels (Vandorpe *et al.*, 1997), suggesting that TRPP3 may contribute to renal Na reabsorption. Of note, although TRPP3 channels over-expressed in *Xenopus* oocytes exhibit high unitary conductance and low sensitivity to amiloride inhibition, these parameters for *in vivo* TRPP3 channels in kidney and other organs might be substantially different because of possible presence of tissue-specific modulatory protein subunits. Thus understanding effects of amiloride on the TRPP3 channel may help to determine its physiological roles in kidney and other tissues.

The mouse orthologue of TRPP3 is deleted in *krd* (kidney and retinal defects) mice, resulting in defects in kidney and retina (Keller *et al.*, 1994;Nomura *et al.*, 1998). TRPP3 may be one of the candidates linked to unmapped human genetic cystic disorders such as dominantly transmitted glomerulocystic kidney disease of post-infantile onset, isolated polycystic liver disease,

and Hajdu-Cheney syndrome/serpentine fibula syndrome (Nomura *et al.*, 1998). Although no evidence showed the TRPP3's direct involvement in ADPKD or ARPKD, a role for TRPP3 in cystogenesis is not excluded, as an interaction between TRPP3 and polycystin-1 exists (Murakami *et al.*, 2005). Co-expression of TRPP3 together with polycystin-1 resulted in the expression of TRPP3 channels on the cell surface, whereas TRPP3 expressed alone was retained with the ER (Murakami *et al.*, 2005). Monolayers formed by ARPKD principal cells of human fetal renal collecting ducts exhibit remarkably higher transepithelial Na reabsorption than control monolayers (Rohatgi *et al.*, 2003; Olteanu *et al.*, 2006). Interestingly, this increased Na movement is partially inhibited by amiloride with relatively low affinity. In contrast, the amiloride-sensitive Na reabsorption is decreased in principal cells isolated from *bpk* ARPKD mice (Veizis *et al.*, 2003). Because the protein mutated in these ARPKD cells does not resemble an ion channel or transporter, we speculate that it may regulate the surface membrane expression and/or function of to-be-identified channels or transporters that are permeable to Na with low sensitivity to amiloride. The regulation could be through physical binding or indirectly through a cascade pathway that links a PKD protein to an ion channel or transporter. Interestingly, cyst growth can be interfered in animal and *in vitro* studies by a number of compounds, in particular, by the use of amiloride and its analogs (Ogborn, 1994).

In summary, TRPP3 may account for amiloride-sensitive cation currents in some tissues and play critical physiological roles in both neuronal and non-neuronal cells, eg in brain, retina and kidney, by mediating amiloride-sensitive, pH-dependent cation fluxes.

Acknowledgements

We thank Dr. Mariusz Klobukowski for help on using the Spartan 4 program.

References

- Basora N, Nomura H, Berger UV, Stayner C, Guo L, Shen X, & Zhou J (2002). Tissue and cellular localization of a novel polycystic kidney disease-like gene product, polycystin-L. *J Am Soc Nephrol* **13**, 293-301.
- Chen XZ, Vassilev PM, Basora N, Peng JB, Nomura H, Segal Y, Brown EM, Reenders ST, Hediger MA, & Zhou J (1999). Polycystin-L is a calcium-regulated cation channel permeable to calcium ions. *Nature* **401**, 383-386.
- Chu XP, Zhu XM, Wei WL, Li GH, Simon RP, MacDonald JF, & Xiong ZG (2003). Acidosis decreases low Ca(2+)-induced neuronal excitation by inhibiting the activity of calcium-sensing cation channels in cultured mouse hippocampal neurons. *J Physiol* **550**, 385-399.
- Clapham DE (2003). TRP channels as cellular sensors. *Nature* **426**, 517-524.
- Dai XQ, Karpinski E, & Chen XZ (2006). Permeation and inhibition of polycystin-L channel by monovalent organic cations. *Biochim Biophys Acta* **1758**, 197-205.
- Delmas P, Nauli SM, Li X, Coste B, Osorio N, Crest M, Brown DA, & Zhou J (2004). Gating of the polycystin ion channel signaling complex in neurons and kidney cells. *FASEB J* **18**, 740-742.
- Doi Y & Marunaka Y (1995). Amiloride-sensitive and HCO₃⁻-dependent ion transport activated by aldosterone and vasotocin in A6 cells. *Am J Physiol* **268**, C762-C770.
- Gilbertson TA, Roper SD, & Kinnamon SC (1993). Proton currents through amiloride-sensitive Na⁺ channels in isolated hamster taste cells: enhancement by vasopressin and cAMP. *Neuron* **10**, 931-942.
- Gonzalez-Perret S, Kim K, Ibarra C, Damiano AE, Zotta E, Batelli M, Harris PC, Reisin IL, Arnaout MA, & Cantiello HF (2001). Polycystin-2, the protein mutated in autosomal dominant polycystic kidney disease (ADPKD), is a Ca²⁺-permeable nonselective cation channel. *Proc Natl Acad Sci U S A* **98**, 1182-1187.
- Hirsh AJ (2002). Altering airway surface liquid volume: inhalation therapy with amiloride and hyperosmotic agents. *Adv Drug Deliv Rev* **54**, 1445-1462.

Huang AL, Chen X, Hoon MA, Chandrashekar J, Guo W, Trankner D, Ryba NJ, & Zuker CS (2006). The cells and logic for mammalian sour taste detection. *Nature* **442**, 934-938.

Ishimaru Y, Inada H, Kubota M, Zhuang H, Tominaga M, & Matsunami H (2006). Transient receptor potential family members PKD1L3 and PKD2L1 form a candidate sour taste receptor. *Proc Natl Acad Sci U S A* **103**, 12569-12574.

Keller SA, Jones JM, Boyle A, Barrow LL, Killen PD, Green DG, Kapousta NV, Hitchcock PF, Swank RT, & Meisler MH (1994). Kidney and retinal defects (Krd), a transgene-induced mutation with a deletion of mouse chromosome 19 that includes the Pax2 locus. *Genomics* **23**, 309-320.

Kleyman TR & Cragoe EJ, Jr. (1988). Amiloride and its analogs as tools in the study of ion transport. *J Membr Biol* **105**, 1-21.

Kleyman TR & Cragoe EJ, Jr. (1990). Cation transport probes: the amiloride series. *Methods Enzymol* **191:739-55.**, 739-755.

Koulen P, Cai Y, Geng L, Maeda Y, Nishimura S, Witzgall R, Ehrlich BE, & Somlo S (2002). Polycystin-2 is an intracellular calcium release channel. *Nat Cell Biol* **4**, 191-197.

Lawonn P, Hoffmann EK, Hougaard C, & Wehner F (2003). A cell shrinkage-induced non-selective cation conductance with a novel pharmacology in Ehrlich-Lette-ascites tumour cells. *FEBS Lett* **539**, 115-119.

Li Q, Liu Y, Shen PY, Dai XQ, Wang S, Smillie LB, Sandford R, & Chen XZ (2003). Troponin I binds polycystin-L and inhibits its calcium-induced channel activation. *Biochemistry* **42**, 7618-7625.

Lilley S, LeTissier P, & Robbins J (2004). The discovery and characterization of a proton-gated sodium current in rat retinal ganglion cells. *J Neurosci* **24**, 1013-1022.

Liu Y, Li Q, Tan M, Zhang Y-Y, Karpinski E, Zhou J, & Chen X-Z (2002). Modulation of the human polycystin-L channel by voltage and divalent cations. *FEBS Lett* **525**, 71-76.

LopezJimenez ND, Cavenagh MM, Sainz E, Cruz-Ithier MA, Battey JF, & Sullivan SL (2006). Two members of the TRPP family of ion channels, Pkd113 and Pkd211, are co-expressed in a subset of taste receptor cells. *J Neurochem* **98**, 68-77.

Murakami M, Ohba T, Xu F, Shida S, Satoh E, Ono K, Miyoshi I, Watanabe H, Ito H, & Iijima T (2005). Genomic organization and functional analysis of murine PKD2L1. *J Biol Chem* **280**, 5626-5635.

Murata Y, Harada K, Nakajima F, Maruo J, & Morita T (1995). Non-selective effects of amiloride and its analogues on ion transport systems and their cytotoxicities in cardiac myocytes. *Jpn J Pharmacol* **68**, 279-285.

Nauli SM, Alenghat FJ, Luo Y, Williams E, Vassilev P, Li X, Elia AE, Lu W, Brown EM, Quinn SJ, Ingber DE, & Zhou J (2003). Polycystins 1 and 2 mediate mechanosensation in the primary cilium of kidney cells. *Nat Genet*.

Nomura H, Turco AE, Pei Y, Kalaydjieva L, Schiavello T, Weremowicz S, Ji W, Morton CC, Meisler M, Reeders ST, & Zhou J (1998). Identification of PKDL, a novel polycystic kidney disease 2-like gene whose murine homologue is deleted in mice with kidney and retinal defects. *J Biol Chem* **273**, 25967-25973.

Ogborn MR (1994). Polycystic kidney disease--a truly pediatric problem. *Pediatr Nephrol* **8**, 762-767.

Olteanu D, Yoder BK, Liu W, Croyle MJ, Welty EA, Rosborough K, Wyss JM, Bell PD, Guay-Woodford LM, Bevenssee MO, Satlin LM, & Schwiebert EM (2006). Heightened epithelial Na⁺-channel-mediated Na⁺ absorption in a murine polycystic kidney disease model epithelium lacking apical monocilia. *Am J Physiol Cell Physiol* **290**, C952-C963.

Rohatgi R, Greenberg A, Burrow CR, Wilson PD, & Satlin LM (2003). Na transport in autosomal recessive polycystic kidney disease (ARPKD) cyst lining epithelial cells. *J Am Soc Nephrol* **14**, 827-836.

Sariban-Sohraby S & Benos DJ (1986). The amiloride-sensitive sodium channel. *Am J Physiol* **250**, C175-C190.

Stoner LC & Viggiano SC (2000). Apical nonspecific cation channels in everted collecting tubules of potassium-adapted ambystoma. *J Membr Biol* **177**, 109-116.

Tytgat J, Vereecke J, & Carmeliet E (1990). Mechanism of cardiac T-type Ca channel blockade by amiloride. *J Pharmacol Exp Ther* **254**, 546-551.

MOL #37150

Vandorpe DH, Chernova MN, Jiang L, Sellin LK, Wilhelm S, Stuart-Tilley AK, Walz G, & Alper SL (2001). The cytoplasmic C-terminal fragment of polycystin-1 regulates a Ca²⁺-permeable cation channel. *J Biol Chem* **276**, 4093-4101.

Vandorpe DH, Ciampolillo F, Green RB, & Stanton BA (1997). Cyclic nucleotide-gated cation channels mediate sodium absorption by IMCD (mIMCD-K2) cells. *Am J Physiol* **272**, C901-C910.

Veizis EI, Carlin CR, & Cotton CU (2003). Decreased amiloride-sensitive Na⁺ absorption in collecting duct principal cells isolated from bpk ARPKD mice. *Am J Physiol Renal Physiol* ..

Wu G, Hayashi T, Park JH, Dixit M, Reynolds DM, Li L, Maeda Y, Cai Y, Coca-Prados M, & Somlo S (1998). Identification of PKD2L, a human PKD2-related gene: tissue-specific expression and mapping to chromosome 10q25. *Genomics* **54**, 564-568.

Footnotes

This work was supported by the Canadian Institutes of Health Research, the Alberta Heritage Foundation for Medical Research and the Kidney Foundation of Canada (to X.-Z.C.). X.-Z.C. is an AHFMR Senior Scholar. X.-Q.D. is a recipient of the AHFMR Studentship. Address reprint requests to: Dr. Xing-Zhen Chen, 729 Medical Science Building, Department of Physiology, University of Alberta, Edmonton, Alberta, T6G 2H7, Canada. Tel: 1-780-492-2294, Fax: 1-780-492-8915, Email: xzchen@ualberta.ca

Legends for Figures

Fig. 1. Effects of amiloride analogs on the uptake mediated by TRPP3 expressed in *Xenopus*

oocytes. **A.** Chemical structures of amiloride and its analogs (from CHEMnetBASE, <http://www.chemnetbase.com>, for amiloride, EIPA and benzamil; from Sigma, <http://www.sigmaaldrich.com>, for phenamil). **B.** Uptake of radioactive ^{45}Ca mediated by TRPP3 channel using the standard NaCl-containing solution, plus 1 mM non-radiolabelled CaCl_2 and radiolabelled ^{45}Ca , in the presence and absence of 500 μM amiloride, 10 μM phenamil, 10 μM benzamil or 100 μM EIPA, respectively. Shown data are averages from six independent measurements. Control uptake level was obtained using H_2O -injected oocytes. '**' indicates very significant inhibition: $P < 0.01$.

Fig. 2. Effects of amiloride analogs on the Ca-activated whole-cell currents mediated by

TRPP3 channel. **A.** The TRPP3-mediated whole-cell currents obtained using the two-microelectrode voltage clamp. Currents carried by Na and Ca were measured at -50 mV in the presence of the standard NaCl-containing solution ('Na') \pm Ca (5 mM) \pm amiloride (500 μM). The duration between consecutive applications of 5 mM Ca was 10 min, for the TRPP3 channels to recover (same in C and E). 'Na + Ca' = the NaCl-containing solution + 5 mM CaCl_2 . 'Amiloride' = 500 μM amiloride. **B.** Averaged current-voltage relationships (I-V curves) in the presence or absence of 500 μM amiloride ($N = 16$), obtained using a voltage ramp protocol (top). **C.** Effects of benzamil on the TRPP3-mediated whole-cell currents under voltage clamp (-50 mV). **D.** Averaged I-V curves in the presence or absence of 1 μM benzamil ($N = 15$). **E.** Effects of 0.3 μM phenamil on the whole-cell currents at -50 mV. **F.** Averaged I-V curves in the presence or absence of 0.3 μM phenamil ($N = 13$). **G.** Averaged concentration-dependent curves for amiloride, EIPA, benzamil and phenamil ($N = 36, 32, 30$ and 28 , respectively). Curves are fits with the Logistic equation (see

Methods). **H.** Concentration-dependent curves for phenamil in the presence (solid triangle, N = 32) or absence (open triangle, same as in panel **G**) of TPeA (0.5 μ M).

Fig. 3. Effects of amiloride analogs on the TRPP3-mediated basal Na currents. A and B.

Representative current recording at -50 mV in an oocyte expressing TRPP3 in the presence or absence of amiloride (500 μ M) (**A**) or phenamil (1 μ M) (**B**). ‘NMDG’ indicates the ‘Na’ solution in which Na was replaced by the equimolar N-Methyl-D-glucamine. **C.** Basal Na currents at -50 mV inhibited by 500 μ M amiloride, 100 μ M EIPA, 10 μ M benzamil or 1 μ M phenamil, in oocytes expressing TRPP3 or H₂O-injected oocytes. **D.** Averaged concentration dependence of normalized basal Na currents at -50 mV for various amiloride analogs. The IC₅₀ values were estimated to be 155 ± 0.01 (N = 23), 12.2 ± 0.01 (N = 18), 2.43 ± 0.01 (N = 22) and 0.28 ± 0.04 μ M (N = 22) for amiloride, EIPA, benzamil and phenamil, respectively.

Fig. 4. Effects of amiloride on TRPP3 single-channel properties. The cell-attached mode of the patch clamp technique was used in these experiments. **A.** Representative recordings (left) and the corresponding density plots (right) at indicated voltages in the presence pipette 123 mM K

(Control) \pm 500 μ M amiloride. The closed levels are indicated by horizontal dashed lines. Shown traces were Gaussian filtered at 200 Hz, using Clampfit 9. The tracings in the presence or absence of amiloride were from the same oocytes. **B.** Averaged (N = 8) NP_o values at various V_m \pm amiloride (500 μ M). A two-way ANOVA analysis produced P < 0.0001 for amiloride and V_m, and P = 0.008 for the amiloride x V_m interaction. **C.** Effects of amiloride on MOT. P = 0.002 for amiloride, P < 0.0001 for V_m, and P = 0.01 for the amiloride x V_m interaction. **D.** Averaged single-channel amplitudes obtained in the presence or absence of amiloride (500 μ M) (N = 15, P > 0.05).

Fig. 5. Effects of EIPA. A. Representative recordings (left) at -120 mV in the presence of 123 mM K (control) in the pipette, plus 0, 0.5, 5, 10, 20, 50 or 100 μ M EIPA, and the corresponding density plots (right). The tracings at different EIPA concentrations were from the same oocytes. **B.**

Concentration-dependent curves for the inhibition of NP_o by EIPA at -120 mV and +120 mV, respectively. Data were averaged from 20 determinations. The curves are fits by the Logistic equation. **C.** Concentration-dependent curves for the inhibition of MOT by EIPA (N = 20).

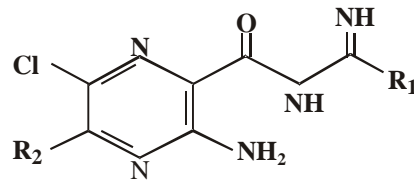
Fig. 6. Effects of benzamil. A. Representative recordings (left) at -120 mV in the presence of benzamil at various concentrations and the corresponding density plots (right), from the same oocytes. **B** and **C.** Concentration-dependent curves for the inhibition of NP_o (N= 24) and MOT (N= 20) by benzamil at -120 and +120 mV, respectively. Each point was averaged from 13 determinations.

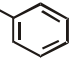
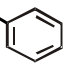

Fig. 7. Effects of phenamil. A. Representative recordings (left) at +100 and -120 mV in the presence of phenamil at various concentrations and the corresponding density plots (right), from the same oocytes. **B** and **C.** Concentration-dependent curves for the inhibition of NP_o (N = 26) and MOT (N = 19) by phenamil at -120 and +120 mV, respectively.

Fig. 8. Effects of amiloride analogs on TRPP3 single-channel parameters. 500 μM amiloride, 100 μM EIPA, 1 μM benzamil and 1 μM phenamil were used in the cell-attached experiments. **A** and **B.** Inhibition of NP_o and MOT at -V_m (N = 15-26) and +V_m (N = 11-20). **C.** Inhibition of mean currents at -120 mV (N = 15-26) and +120 mV (N = 11-20). **D.** IC₅₀ values for amiloride and its analogs as a function of their molecular size. Ca-activated whole-cell currents were used to determine the IC₅₀ values averaged from 36, 25, 30 and 28 measurements for amiloride, EIPA, benzamil and phenamil, respectively. The diameters of amiloride, EIPA, benzamil and phenamil are 9.9, 12.0, 13.8 and 14.2 Å (unfolded model), respectively.

Figure 1

A



	AM	Benzamil	EIPA	Phenamil
R ₁	-NH ₂	-NH- 	-NH ₂	-NH- 
R ₂	-NH ₂	-NH ₂		-NH ₂

B

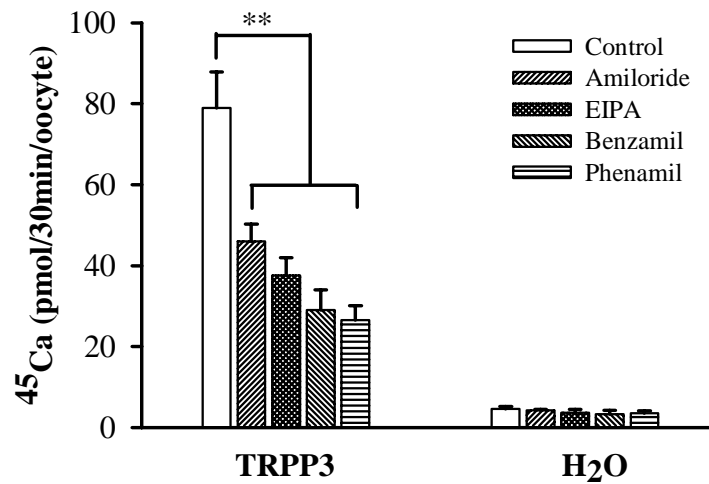


Figure 2

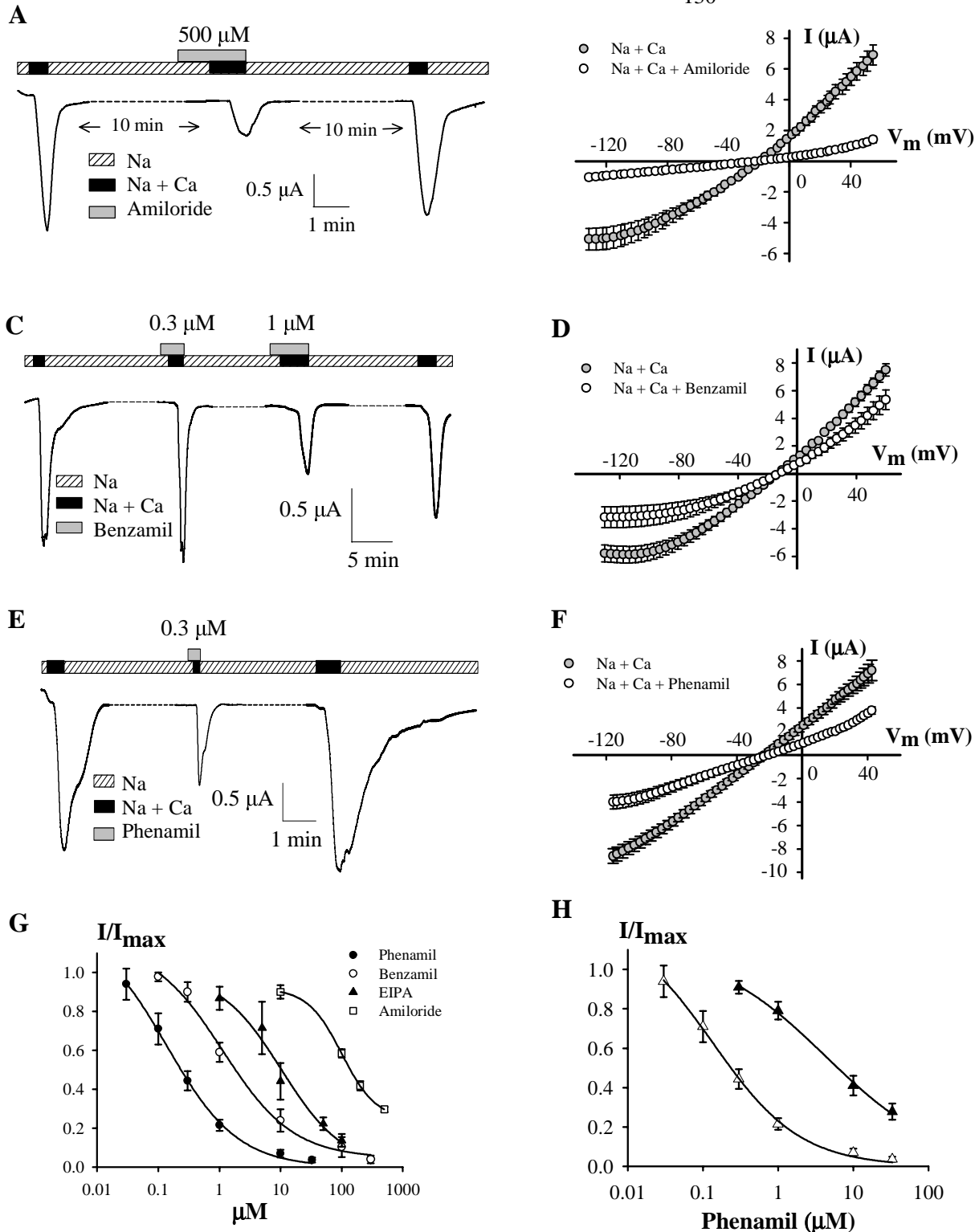


Figure 3

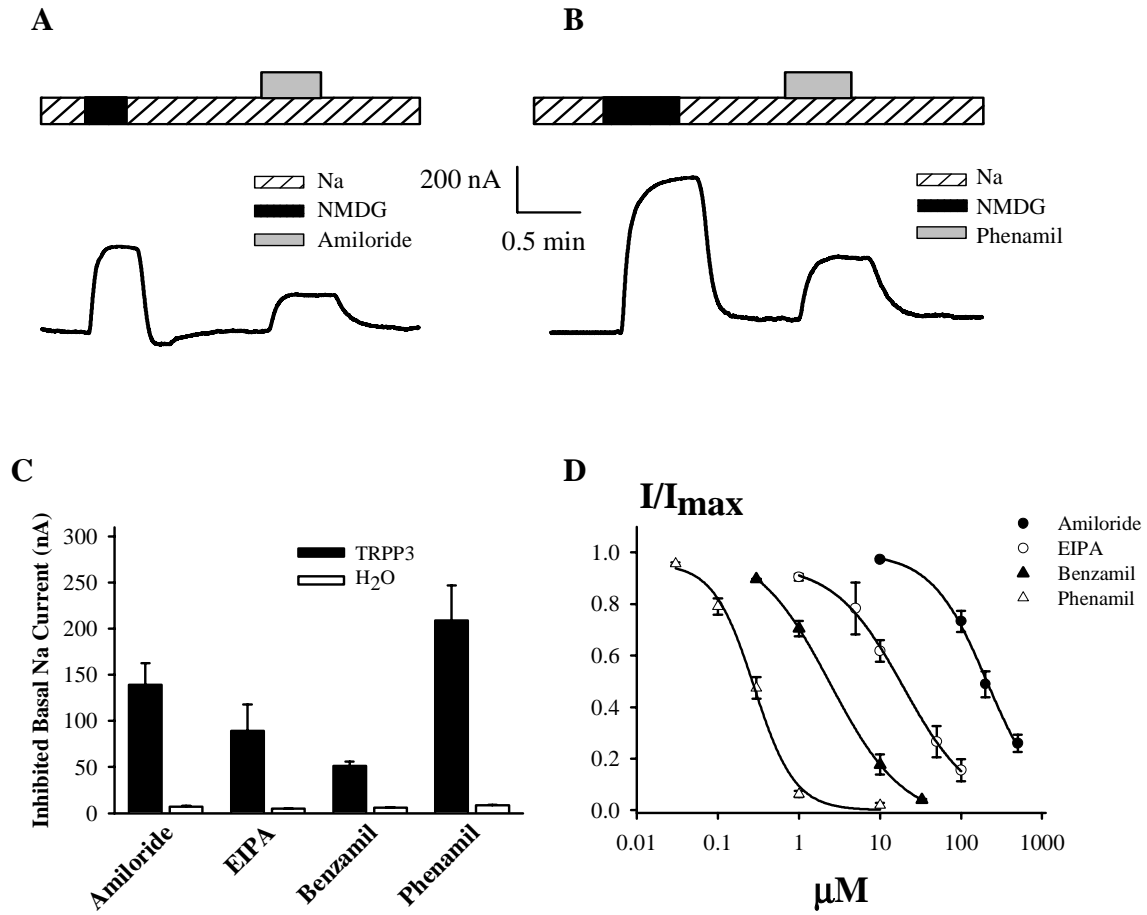


Figure 4

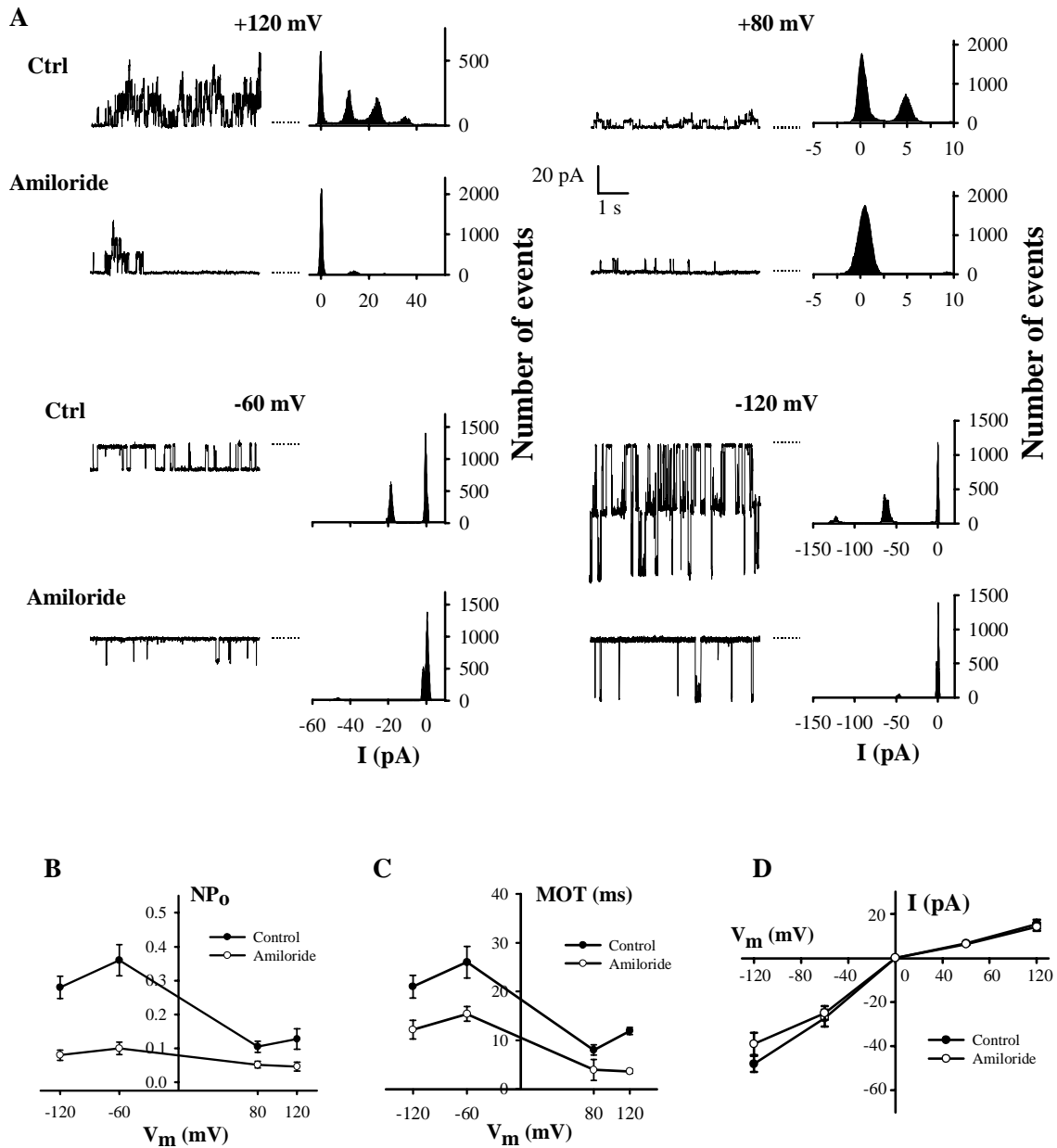


Figure 5

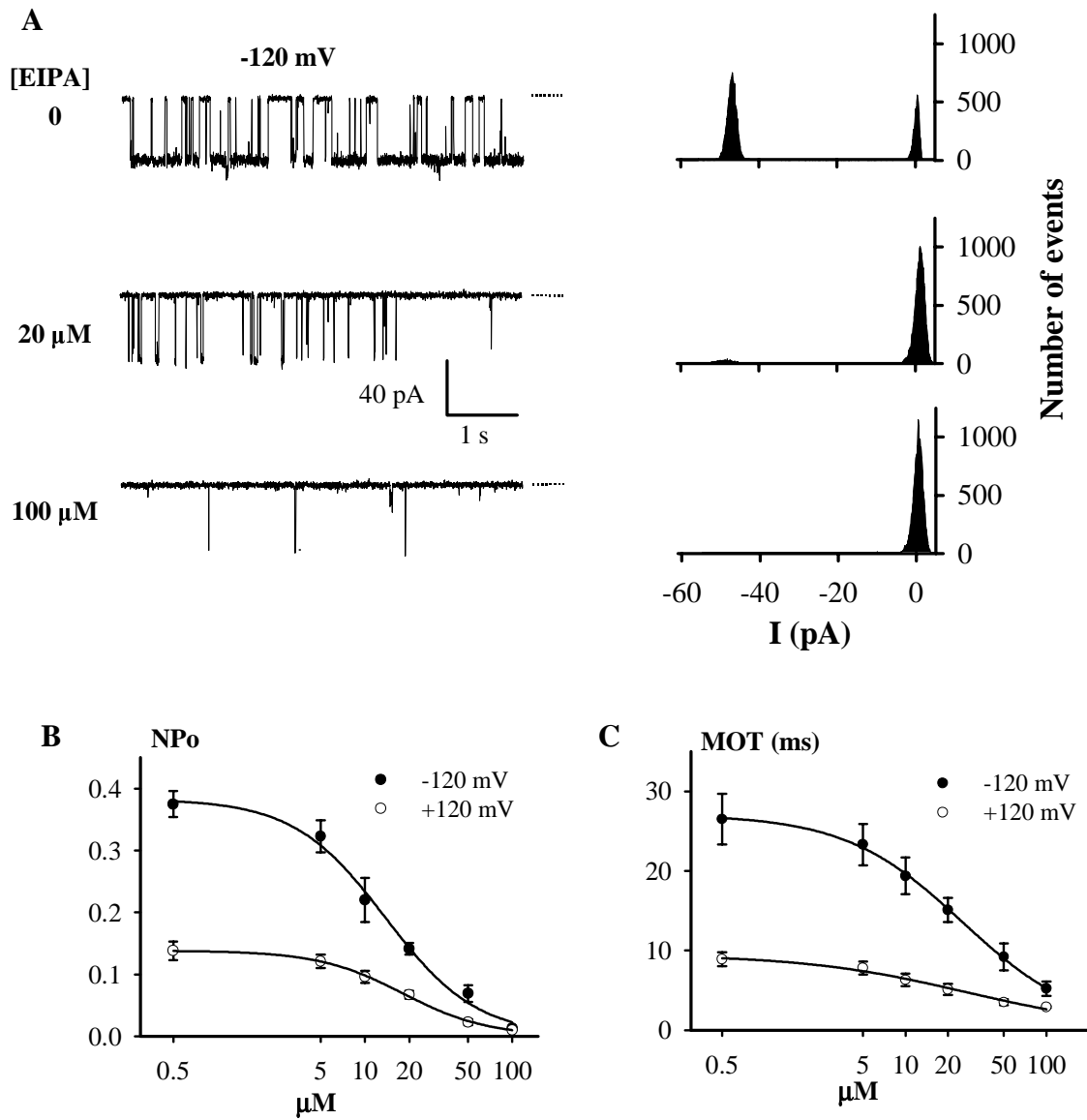


Figure 6

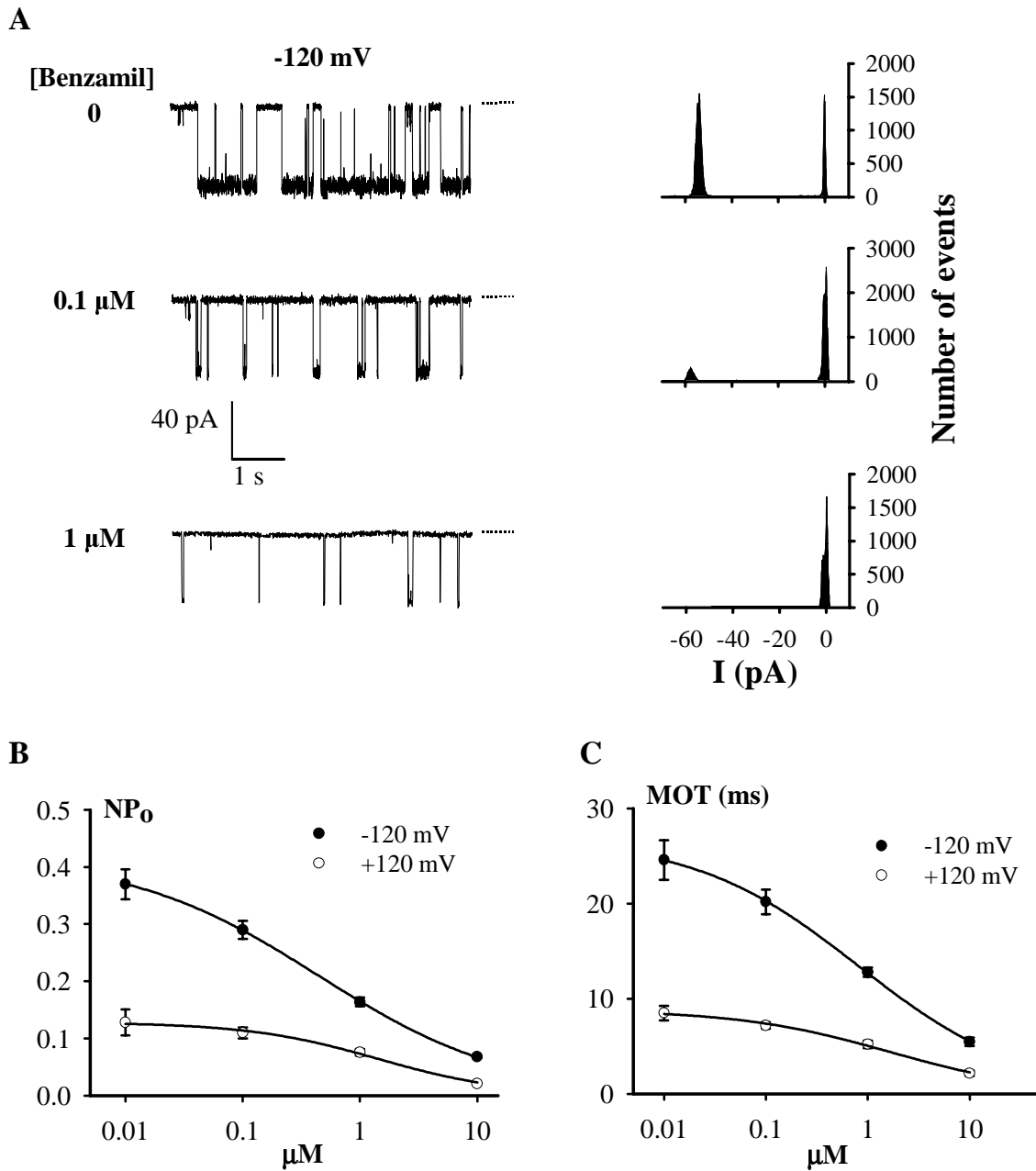


Figure 7

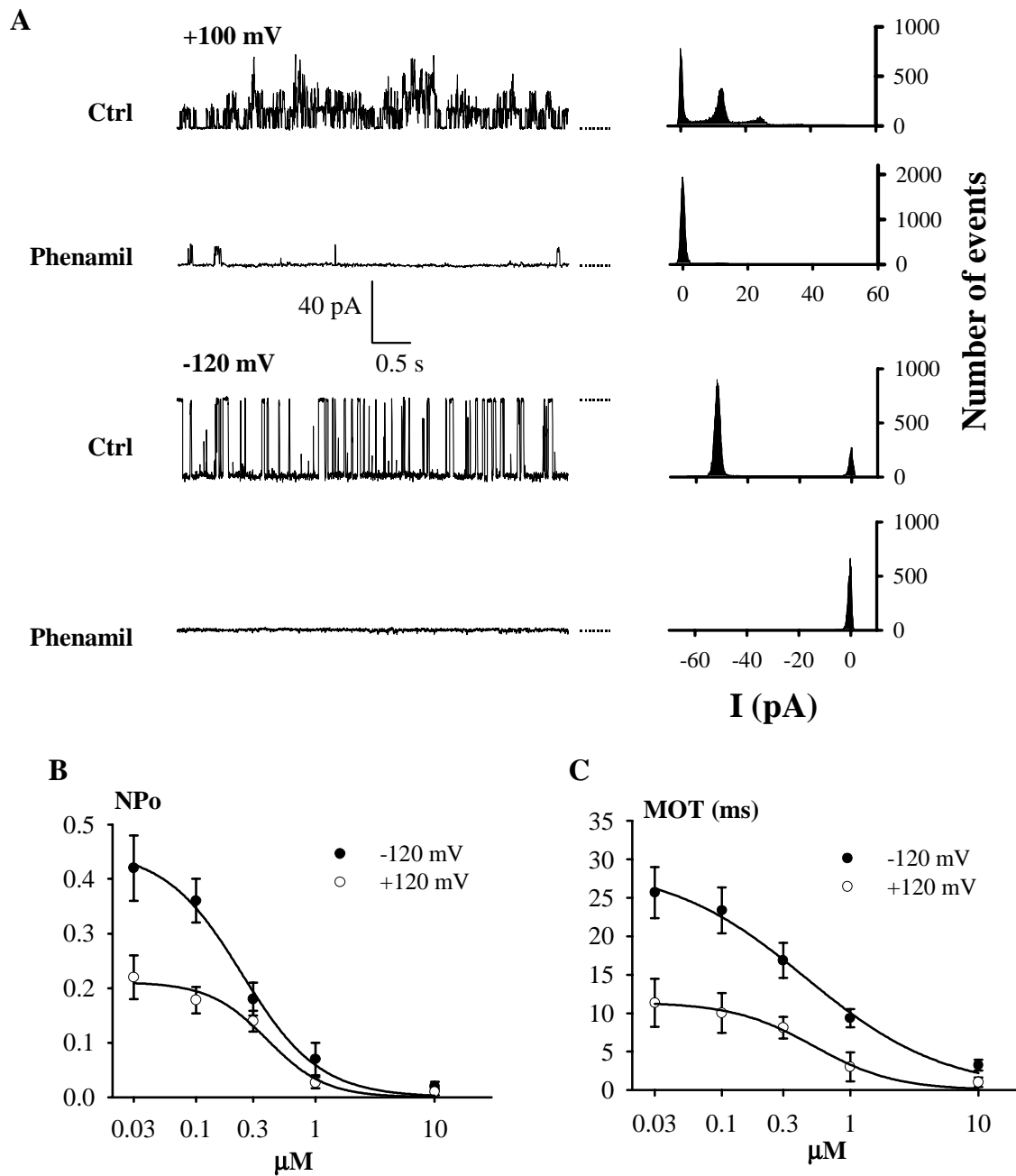


Figure 8

